Chemical Physics 22 (1977) 175–181

A COMPARISON OF THE THEORETICAL AND EXPERIMENTAL ELECTRON DENSITY DISTRIBUTION IN THE CYANIDE AND THIOCYANATE GROUP

J.W. BATS and D. FEIL
Chemical Physics Laboratory, Twente University of Technology, Enschede, The Netherlands

Received 14 January 1977

Electron density distributions, derived from ab initio molecular wavefunctions, have been calculated for CN^- and SCN^- ions. From these dynamic densities were calculated assuming rigid body thermal vibrations of the molecules. Comparison with the difference density in $NaCN \cdot 2H_2O$, NaSCN and NH_4SCN, observed by X-ray diffraction, is fair. Remaining differences between theory and experiment are discussed. The Hartree–Fock method gives a better correspondence with the observed electron density distribution in the thiocyanate ion than the Hartree–Fock–Slater method.

1. Introduction

The growing interest in the determination of the electron density distribution in various compounds by means of X-ray diffraction, calls for a comparison of experimental and theoretical electron densities. The theoretical electron density, derived from molecular wavefunctions, however, corresponds to the density of a molecule at rest, while in the X-ray diffraction experiment the electron density is observed as a time-average over the thermal vibrations in the crystal. The desired comparison of theory and experiment, therefore, requires an averaging of the theoretical electron density over the different modes of vibration.

The thermal motion of the atoms in molecular crystals can, in good approximation, be subdivided into two groups: (a) internal vibrations of the molecule; (b) external vibrations of the molecule as a rigid body, described by coupled rigid body translations and librations. For many structures the observed thermal parameters can be adequately analysed in terms of rigid body motion, whereby a part of the internal vibrations may be absorbed by the rigid body model.

A convolution of the static, theoretical density with a distribution function describing the motion of the molecule [1] is straightforward as long as only uncoupled rigid body translations and librations are considered to contribute to the motion of the molecule. When the internal vibrations of the molecule are included, the method becomes less simple. In that case molecular wavefunctions have to be calculated for a large number of molecular geometries and the result of the internal vibrations accounted for by an averaging over these geometries.

An extensive study of the thermal smearing of the electron density in an acetylene model structure, including internal and rigid body vibrations, has been made by Ruysink and Vos [2]. They conclude that the internal vibrations are not important to describe the time-average electron density in this particular case. Thermally smeared theoretical densities, based on rigid body vibrations have been reported by a number of authors [3,4,5]. In the present work time-average, theoretical electron densities, based on a rigid body model for the thermal motion, will be calculated for the CN^- and SCN^- ions. Comparison will be made with experimental electron densities for these groups as observed in $NaCN \cdot 2H_2O$ at 150 K, NaSCN at 150 K and 81 K and NH_4SCN at 81 K. The first two compounds have been studied by X-ray diffraction alone [6,7], the last one by a combined X-ray and neutron diffraction study [8].

2. Method

2.1. General case

In this work it will be assumed that only rigid body vibrations contribute to the thermal motion of the atoms in the crystal. Then the dynamic or time-average theoretical density is obtained by the convolution:

$$\rho_d(r) = \int \rho_{st}(r-u)\, P(u)\, du\,, \qquad (1)$$

with $\rho_d(r)$: the dynamic density, $\rho_{st}(r)$: the static density and $P(u)$: a function describing the probability that point $(r-u)$ is displaced over a distance u from its equilibrium position.

The correlation between the translational and librational modes of vibration is neglected. This implies that the S-tensor in the rigid body description of Schomaker and Trueblood [9] is zero, in which case the rigid body model reduces to the TLX model of Pawley [10]. $P(u)$ can then be considered as a convolution of probability density functions for the translational and librational motion:

$$P(u) = P_{tr}(u^{tr}) * P_{lib}(u^{lib})\,. \qquad (2)$$

(The symbol * denotes convolution). Thus eq. (1) can be written as:

$$\rho_d(r) = \iint \rho_{st}(r - u^{tr} - \mathbf{D}\cdot r)\, P_{tr}(u^{tr})\, P_{lib}(\omega)\, du^{tr}\, d\omega. \qquad (3)$$

The tensor D is described by Schomaker and Trueblood [9] and corresponds to a rotation $|\omega|$ about vector ω such that $\mathbf{D}\cdot r = u^{lib}$. The probability density functions for translation and libration are in the harmonic approximation given by:

$$P_{tr}(r) = (2\pi)^{-3/2}\, |\mathbf{T}^{-1}|^{1/2} \exp(-\tfrac{1}{2} r^{T} \mathbf{T}^{-1} r)\,, \qquad (4a)$$

$$P_{lib}(\omega) = (2\pi)^{-3/2} |\mathbf{L}^{-1}|^{1/2} \exp(-\tfrac{1}{2}\, \omega^{T} \mathbf{L}^{-1} \omega)\,, \qquad (4b)$$

with T and L the translation and libration tensors defined by several authors [9,10].

Several methods have been proposed to deal with eq. (3). Ruysink and Vos [2] and Scheringer and Reitz [11] describe an analytic evaluation of the integrals, in which case the static electron density has to be expressed in terms of gaussian basis functions. Hase et al. [4] and Stevens et al. [5] evaluate eq. (3) in reciprocal space. The advantage of the latter method is that $\rho_d(r)$ will contain the series termination effect of the Fourier summation, which is also present in the experimental electron density distribution.

In the present work we evaluate eq. (3) by numerical integration in direct space. This method may be less efficient in computing time than the alternative methods, but has the advantage that the expressions remain fairly simple.

2.2. Special case

In the present study the assumption is made that the molecular axis corresponds to a principal axis of the translation tensor T and that the rigid body motion can be described by three principal modes of translation and two modes of libration about axes normal to the molecular axis. The observed thermal parameters [6–8] are well described by this model. Furthermore it is assumed that the thermal motion is isotropic in the direction normal to the bond axis. This second condition is not fulfilled but no significant errors are expected to be made if the time-average density is calculated only along the molecular axis.

Four parameters are then required to describe the rigid body motion of the molecule: $T_{\parallel}, T_{\perp}$: the mean square displacements of translation in axial and radial direction, L: the mean square amplitude of libration about axes normal to the bond axis, X: the center of libration, taken on the bond axis.

When the time-average density is calculated along the molecular axis, taken as the x axis, only, the rotational symmetry of the static density about the molecular axis can be taken into account. The dynamic density is then, in cylindrical coordinates x and r, given by:

$$\rho_d(x_1) = \int_{x=-\infty}^{\infty} \int_{r=0}^{\infty} \rho(x_1 - x, -r) P(x) P(r) 2\pi r\, dx\, dr\,, \qquad (5a)$$

with

$$P(x) = (2\pi T_{\parallel})^{-1/2} \exp[-x^2/(2T_{\parallel})]\,, \qquad (5b)$$

and

$$P(r) = (2\pi T_{\perp})^{-1} \exp[-r^2/(2T_{\perp})]\,. \qquad (5c)$$

The static density has been calculated in a two-dimen-

sional grid. The time-average density was obtained by replacing the integrals in eq. (5a) by summations over the gridpoints.

As the librational amplitudes are small for the thiocyanates studied in this work and since the time-average density is only calculated along the bond axis, a further simplification can be made by replacing the librational motion by a linear vibration with mean square displacement:

$$\langle u_Q^2 \rangle = (x - X)^2 L \,. \qquad (6)$$

This assumption was found to give negligible errors in the model calculation on acetylene [2]. Now it is easily shown that the averaging of the static density over both the translations and the linear vibrations described by eq. (6) is again achieved by eqs. (5a)–(5c) when $T_\perp$ is replaced by $T_\perp + \langle u_Q^2 \rangle$.

3. Application

The parameters describing the rigid body motion of the CN and SCN group in the crystal structures of $NaCN \cdot 2H_2O$, NaSCN and NH_4SCN, are reported in table 1. For the CN group in $NaCN \cdot 2H_2O$ the libration cannot be derived from the experimental thermal parameters. In this case the thermal motion of the atoms has to be divided over a translational and a librational motion in an arbitrary way. A libration with $L = 0.010$ rad^2 about the center of the CN bond has been adopted.

The static electron density of the CN^- and SCN^- ions has been derived from Hartree–Fock molecular wavefunctions, given by Bonaccorsi et al. [12] and McLean and Yoshimine [13] respectively. The geometry adopted by McLean and Yoshimine for the SCN^- group ($r_{CS} = 1.561$, $r_{CN} = 1.217$ Å) is somewhat different from the geometry observed in NaSCN and NH_4SCN ($r_{CS} = 1.648$, $r_{CN} = 1.176$ Å) which may affect the agreement between the theoretical and experimental electron density. A second molecular wavefunction has been calculated for the SCN^- group with the experimental geometry and using the Hartree–Fock–Slater method [17]. The Hartree–Fock–Slater method was found to give deformation densities for CO and N_2 very similar to the Hartree–Fock method [15,18], but has not yet been tested for molecules containing second-row elements. For this reason little can be said about the expected accuracy of this wavefunction and a comparison with an experimental electron density is very desirable. Both the HF and HFS calculations are based on extended basis sets consisting of double zeta + polarization functions, supposedly adequate for quantitative electron density studies [18].

The static and dynamic total electron density of the CN^- ion and the experimental total electron density in $NaCN \cdot 2H_2O$ are shown in fig. 1. The effect of the thermal motion on the static electron density is considerable. The peaks at the atomic positions reduce to about 2% of their static values. The experimental density shows a considerable deviation from the dynamic density. The discrepancies are especially pronounced at places with the steepest curvature of the dynamics density and can be attributed to the series termination in the Fourier synthesis of the experimental density. Including a larger number of Fourier terms increases the agreement between the experimental and theoretical density, as shown in fig. 1.

A different situation occurs in fig. 2, where the theoretical valence density of the CN^- group is compared with the valence density observed in $NaCN \cdot 2H_2O$. The valence density is obtained by subtracting from the molecular electron density atomic core densities, based on Clementi's atomic orbitals [14]. In this case excellent agreement is found between

Table 1
Rigid body parameters for the CN and SCN group

Structure	Temperature (K)	$T_\parallel$(Å^2)	$T_\perp$(Å^2)	L(rad^2)	X(Å)
$NaCN \cdot 2H_2O$	150	0.017	0.026	0.0100	0.58 a)
NaSCN	150	0.013	0.015	0.0035	0.49 b)
NaSCN	81	0.007	0.009	0.0017	0.58 b)
NH_4SCN	81	0.009	0.011	0.0020	0.75 b)

a) Center of CN bond. b) Point in CS bond at distance X from carbon atom.

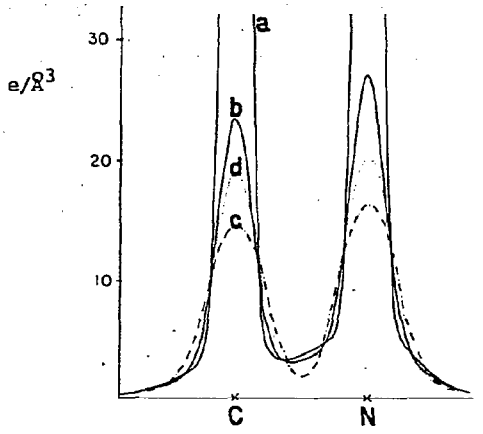

Fig. 1. The total density in the CN^- group: (a) the static density; (b) the dynamic density; (c) the density observed in $NaCN \cdot 2H_2O$ ($\sin\theta/\lambda \leq 0.75$ Å^{-1}); (d) the density observed in $NaCN \cdot 2H_2O$ ($\sin\theta/\lambda \leq 0.92$ Å^{-1}).

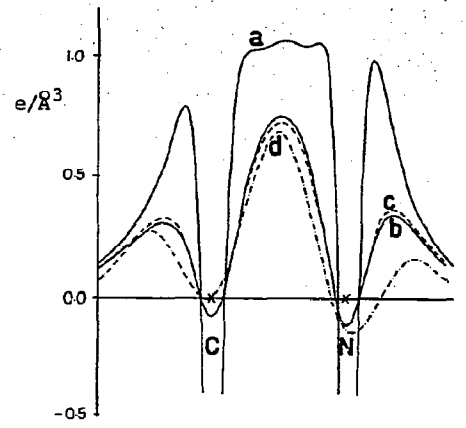

Fig. 3. The deformation density in the CN^- group: (a) the static density; (b) the dynamic density; (c) the dynamic density neglecting librations; (d) the density observed in $NaCN \cdot 2H_2O$.

theory and experiment and it is suggested that the series termination error of the valence density is small in agreement with the smooth curvature of the dynamic valence density.

Generally considered in electron density studies is the deformation density, obtained by subtracting from the molecular electron density an atomic electron density derived from atomic orbitals. Clementi's atomic orbitals [14] have been used to obtain the Hartree–Fock deformation density of CN^- and SCN^-, Hartree–Fock–Slater atomic orbitals for the Hartree–Fock–Slater deformation density of SCN^-.

The static and dynamic deformation density of CN^- is shown in fig. 3, together with the experimental deformation density in $NaCN \cdot 2H_2O$. In figs. 4 and 5 the theoretical deformation density of the SCN^- group, obtained from respectively the Hartree–Fock–Slater and Hartree–Fock calculation, is compared with the deformation density observed in NH_4SCN. The Hartree–Fock deformation density of SCN^- is compared in figs. 6 and 7 with the deformation density observed in NaSCN at 150 K and 81K respectively. Unless mentioned otherwise, the experimental electron density in each figure is based on the X-ray data with $\sin\theta/\lambda \leq 0.75$ Å^{-1}.

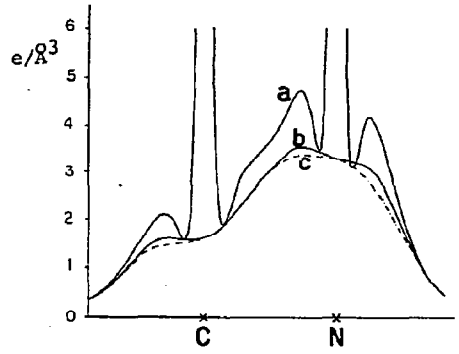

Fig. 2. The valence density in the CN^- group: (a) the static density; (b) the dynamic density; (c) the density observed in $NaCN \cdot 2H_2O$ ($\sin\theta/\lambda \leq 0.75$ Å^{-1}).

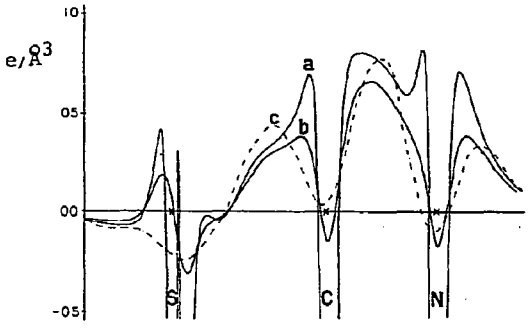

Fig. 4. The Hartree–Fock–Slater deformation density in the SCN^- group: (a) the static density; (b) the dynamic density; (c) the density observed in NH_4SCN.

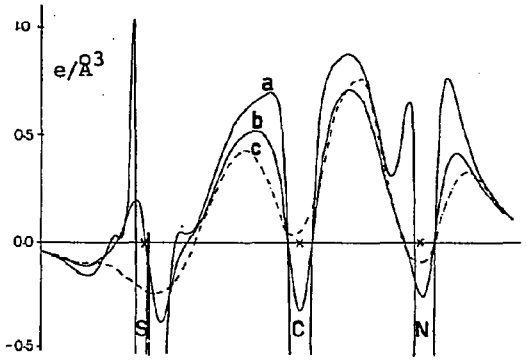

Fig. 5. The Hartree–Fock deformation density in the SCN^- group: (a) the static density; (b) the dynamic density; (c) the density observed in NH_4SCN.

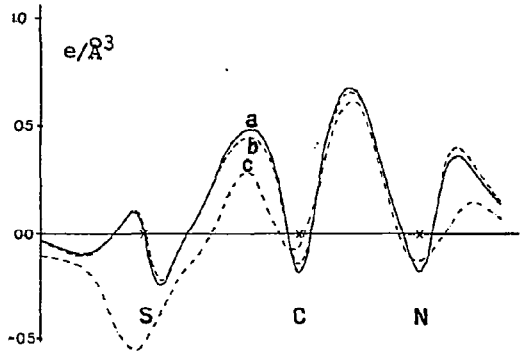

Fig. 6. The deformation density in the SCN^- group: (a) the dynamic density; (b) the dynamic density neglecting librations; (c) the density observed in NaSCN at 150 K.

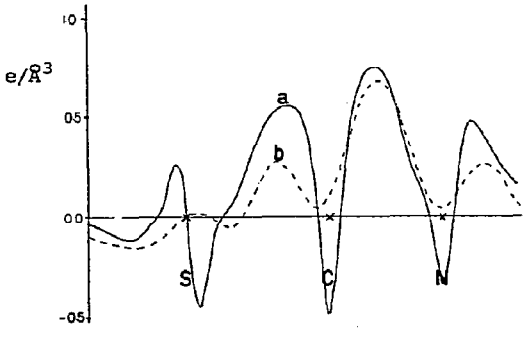

Fig. 7. The deformation density in the SCN^- group: (a) the dynamic density; (b) the density observed in NaSCN at 81 K.

The thermal smearing results in a considerable flattening of the deformation density; the maximum peak heights in the bond and lone pair regions in CN^-, for example, are reduced to about 75% and 40% of their static values, respectively. The very deep cusps at the atomic sites have almost disappeared as a result of the smearing. Very similar results have been reported in the model calculation on acetylene [2].

In order to study the influence on the dynamic deformation density of the arbitrarily chosen librational parameter in $NaCN \cdot 2H_2O$, a calculation with L = 0.0 rad^2 and $T_\perp$ = 0.029 Å^2 is included in fig. 3 (curve c). The maximum difference is only 0.02 e/Å^3 and therefore negligible in view of the standard deviation generally obtained in experimental electron density studies (0.03–0.06 e/Å^3 in the bonding regions). A similar result is found for the SCN^- group. The dynamic deformation density for NaSCN at 150 K, neglecting the libration by taking L = 0.0 rad^2 and $T_\perp$ = 0.020 Å^2, has been included in fig. 6. The effect on the deformation density appears again to be very small and not significant with respect to the experimental errors in the deformation density.

Although the Hartree–Fock and Hartree–Fock–Slater deformation densities of SCN^- are qualitatively very similar, there is a quantitative difference. It is evident from figs. 4 and 5 that the experimental deformation density in NH_4SCN fits the shape of the Hartree–Fock density better than the Hartree–Fock–Slater one does. Therefore only the Hartree–Fock density has been considered in the comparison with NaSCN.

Although the Hartree–Fock deformation density of the CN^- and SCN^- groups shows a fair resemblance with the deformation density observed in $NaCN \cdot 2H_2O$, NH_4SCN and NaSCN, there are a number of striking differences. The nitrogen lone pair peaks and CS bond peaks are systematically lower in the experimental than in the theoretical maps. Moreover it is found that temperature reduction has less effect on the experimental deformation density of NaSCN than the theoretical calculation would indicate. These differences may be related to systematic effects in the treatment of the theoretical and experimental data and will be discussed in more detail in the next section.

4. Discussion

A number of factors may affect the comparison of the time-average theoretical and the experimental electron density:

The lack of accurate atomic parameters. The atomic parameters in the $NaCN \cdot 2H_2O$ and NaSCN structures have been obtained by least-squares fitting of the X-ray intensities collected at high diffraction angles ($\sin\theta/\lambda > 0.65$ Å^{-1}). Lone pair electrons, however, are generally found to contribute to these atomic parameters in the least-squares refinements [16]. The low nitrogen lone pair peaks observed in $NaCN \cdot 2H_2O$ and NaSCN can be attributed to this effect. The experimental deformation density in the CN bonds in these compounds, however, is in excellent agreement with the theoretical density. This suggests that the errors in the positional and thermal parameters cancel in this region while they may accumulate in the lone pair region. Atomic parameters from neutron diffraction would eliminate this error as in the case of NH_4SCN.

Series termination effect. The finite number of terms in the Fourier synthesis of the experimental electron density leads to an underestimation of the electron density with the steepest curvature as illustrated in fig. 1. In the deformation density this effect is expected to be especially pronounced near the atomic positions. It may be responsible for the fact that the experimental deformation density is less dependent on a temperature reduction than the theoretical calculation indicates (see figs. 6 and 7). As both thermal smearing and series termination mostly affect the density regions with the steepest curvature, the gain in detail obtained by temperature reduction in the X-ray diffraction experiment may be partly lost by an increase in the series termination effect. A thermal smearing analysis in reciprocal space [4,5] will be needed to confirm this suggestion.

X-ray scale factor. A scale factor has been applied to the X-ray data to bring the observations on an absolute scale. The uncertainty in the scale factor is estimated at about 1% and will result in errors in the observed deformation density near the atomic positions. These errors are about 0.15 and 0.35 e/Å^3 at the positions of the first and second row atoms, and are most likely responsible for the behaviour of the experimental density in the region near the S-atom in fig. 6. As no better estimates of the X-ray scale factor are presently available [19], these errors cannot yet be reduced.

Incorrect geometry. The Hartree–Fock calculation of the SCN^- ion is based on a structure with a shorter CS bond length than the experimental one. This may be responsible for the low peak-height in this bond in the experimental maps.

Charge transfer and packing effects. Packing effects were found to have little effect on the deformation density in the nitrate ion in a model calculation by de With et al. [20]. The charge transfer between cations and anions in the crystal structure, however, can affect the electron density. A net charge of −1.0 electron has been assigned to the anions in the quantum theoretical calculation, whereas a charge density analysis on the experimental data indicated that values of −0.5, −0.3 and −0.6 electron are more appropriate in case of $NaCN \cdot 2H_2O$, NaSCN and NH_4SCN, respectively [6–8].

Summarising these results, it can be concluded that the Hartree–Fock method gives a better representation of the electron density distribution in the thiocyanate ion than the Hatree–Fock–Slater method. There is a general agreement between the experimental and the time-average theoretical electron density, based on Hartree–Fock calculations. Significant differences remain and have been related to the treatment of the theoretical and experimental data. Further studies of the time-average electron density should be made in reciprocal space rather than in direct space.

References

[1] C.A. Coulson and M.W. Thomas, Acta Cryst. B27 (1971) 1354.
[2] A.F.J. Ruysink and A. Vos, Acta Cryst. A30 (1974) 497.
[3] R.B. Helmholdt, Thesis, University of Groningen (1975).
[4] H.L. Hase, H. Reitz and A. Schweig, Chem. Phys. Letters 39 (1976) 157.
[5] E.D. Stevens, J. Rys and P. Coppens, Acta Cryst. A33 (1977) 333.
[6] J.W. Bats, Acta Cryst. B33 (1977) 466.
[7] J.W. Bats, P. Coppens and A. Kvick, Acta Cryst. B33 (1977), to be published.
[8] J.W. Bats and P. Coppens, Acta Cryst. B33 (1977), to be published.
[9] V. Schomaker and K.N. Trueblood, Acta Cryst. B24 (1968) 63.
[10] G.S. Pawley, Acta Cryst. 16 (1963) 1204.

[11] C. Scheringer and H. Reitz, Acta Cryst. A32 (1976) 271.
[12] R. Bonaccorsi, C. Petrongolo, E. Scrocco and J. Tomasi, Chem. Phys. Letters 3 (1968) 473.
[13] A.D. McLean and M. Yoshimine, IBM J. Res. Develop. 12 (1968) 206, suppl.
[14] E. Clementi, IBM J. Res. Develop. 9 (1965) 2, suppl.
[15] W. Heyser, A.Th. van Kessel and E.J. Baerends, Chem. Phys. 16 (1976) 371.
[16] P. Coppens, Acta Cryst. B30 (1974) 255.
[17] E.J. Baerends, D.E. Ellis and P. Ros, Chem. Phys. 2 (1973) 41.
[18] G. de With and D. Feil, Chem. Phys. Letters 30 (1975) 279.
[19] E.D. Stevens and P. Coppens, Acta Cryst. A31 (1975) 614.
[20] G. de With, D. Feil and E.J. Baerends, Chem. Phys. Letters 34 (1975) 497.